Photophysical characterization and BSA interaction of the direct ring carboxy functionalized unsymmetrical NIR cyanine dyes

Photophysical characterization and BSA interaction of the direct ring Carboxy functionalized unsymmetrical NIR cyanine dyes

Maryala Saikiran*, Daisuke Sato, Shyam S. Pandey*, Takeshi Ohta, Shuzi Hayase and Tamaki Kato*

Graduate School of Life Science and System Engineering, Kyushu Institute of Technology, 2-4 Hibikino, Wakamatsu-Ku, Kitakyushu-Shi, Fukuoka, Japan, 808-0196

Email: msaikiran87@gmail.com, shyam@life.kyutech.ac.jp.

ABSTRACT

Novel near infrared (NIR) sensitive unsymmetrical cyanine dyes bearing direct –COOH functionalized indole ring were synthesized, characterized and subjected to photophysical investigations. These unsymmetrical cyanine dyes were then subjected to investigate their interaction with bovine serum albumin (BSA) as a model protein in Phosphate buffer solutions. Apart from NIR absorption and emission with high molar extinction coefficients they exhibit a blue shift in PBS solution owing to their enhanced dye aggregation. Interaction of these dyes with BSA leads to not only enhanced emission intensity but also bathochromically shifted absorption maximum due to formation of dye-BSA conjugate. These dyes bind strongly with BSA having about an order of magnitude higher binding constant as compared to the typical cyanine dyes. Amongst the unsymmetrical cyanine dyes investigated in this work one bearing substituents like Iodo and carboxylic acid in the terminal Indole rings (UCD-3) exhibited highest association with the BSA having very high binding constant 1.01 x 10^7 M^{-1}.

1. Introduction

Biosensors having the fast, accurate and sensitive detection play a dominant role and attracted huge interest of scientific community in order to provide high quality of life by early disease diagnosis (1, 2). Amongst various biosensors, one based on fluorescence detection technique especially emitting fluorescence signals in the near infra-red (NIR) region bear profound techno-scientific interests. This is attributed to the fact that fluorescence signals in the NIR (700 nm-900 nm) bear least auto-fluorescence associated with background arising from the biological samples like blood, serum and urine etc. proving relatively highly sensitive detection capabilities [3, 4]. In this context, polymethene class of cyanine dyes have attracted a great attention owing to their very high molar extinction coefficients, small Stokes shift and tunability of optical absorption and emission from visible to IR wavelength region by judicious molecular design [5]. Their fluorescence can be readily detected from deep tissues by commercially available imaging modalities making them strong contender for the bio-imaging applications (6-8). Therefore, application of NIR sensitive organic dyes in optical imaging and bio-diagnosis has emerged as potential candidate due to its low energy radiation, non-invasive nature and high sensitivity (9-11).

Cyanine dyes are a unique class of charged chromophores with conjugated polymethene framework consisted of two quaternized nitrogen-containing heterocyclic rings linked together with an intermediate polymethene bridge (12). Cyanine dyes have been used in varied applications such as fluorescent probes in luminescent materials for labelling (13), analyte responsive fluorescent probes (14) and in optoelectronics (15). Wavelength tunable fluorescence emission and

good fluorescence quantum yield enable the cyanine dyes to detect low concentrations of analytes (16). Recent investigations on cyanine dyes have demonstrated that unsymmetrical cyanine dyes are more pronounced and gained much interest due to their excellent nucleic acid staining properties (17). Synthetic versatility due to variable central methene units and availability of huge number of aromatic and heterocyclic terminal functionalities, considerable quantum yield, good tissue penetration, lower noise due to auto fluorescence and possibility of simultaneous multicolor and multi-target imaging enables the cyanine dyes for the utmost interest as fluorescent probes/labels (18, 19).

This article describes the detailed synthesis and photophysical characterization of representative unsymmetrical NIR cyanine dyes bearing direct carboxyl functionalized indole ring. At the same time other terminal indole ring were substituted with electron donating –OH and electronic withdrawing –I groups. In order to explore their potential application as fluorescent probes to sense protein in phosphate buffer solution (PBS), these dyes were subjected to investigations pertaining to their interaction using Bovine serum albumin (BSA) as a model protein. These newly designed dyes bearing -COOH functionalized indole ring provide the capability of covalent coupling with biomolecules such as peptides, oligonucleotides and proteins to enhance their application potential as florescence probes.

2. Experimental

2.1 Materials and Methods

All the chemicals for synthesis and photophysical characterization are of analytical or spectroscopic grade and used as received. Synthesized unsymmetrical cyanine dyes and dye intermediates were analysed by MALDI-TOF/FAB-mass spectroscopy in positive ion monitoring mode and nuclear magnetic resonance spectroscopy (NMR 500MHz for ^{1}H NMR and 125 MHz for the ^{13}C NMR) for structural elucidation. Electronic absorption spectroscopic investigations in solution state were made using UV-visible-NIR spectrophotometer (JASCO V-530 UV/VIS spectrophotometer). At the same time, fluorescence emission spectrum was also recorded using fluorescence emission spectroscopy (JASCO FP-6600 spectrophotometer).

2.2 BSA Interactions

The protein (BSA)-dye interactions were conducted using phosphate buffer solution (PBS, 0.1 M at pH 7.4) and cyanine dye solutions (2μM), prepared by the addition of 100 μl of 0.1 M dye solution in DMF to the various concentrations of PBS/BSA solutions in the concentration range of (0-10 μM). The final solutions were stirred at room temperature before recording the respective electronic absorption and fluorescence emission spectra. To compare the interactions between protein and dye, the apparent binding constants (K_a) were also calculated from fluorescent titrations of dyes at 25^0C. Considering BSA/dye association in 1:1 ratio, the constant K_a was calculated using the equation 1 (20).

$$\frac{1}{(F_x - F_0)} = \frac{1}{(F_\infty - F_0)} + \frac{1}{K_a[BSA]} \frac{1}{(F_\infty - F_0)} \quad [1]$$

Where, F_0, F_X, and F_∞ are the fluorescence intensities of dyes in the absence, presence of BSA and at a concentration of complete interaction, respectively, while [BSA] is the protein concentration. Equation [1] can be modified as

$$\frac{(F_\infty - F_0)}{(F_x - F_0)} = 1 + \frac{1}{K_a[BSA]} \quad [2]$$

The binding constant values (K_a) for the interaction between the BSA and cyanine dyes were calculated from the slopes of the corresponding plots between the $(F_\infty - F_0)/(F_X - F_0)$ as a function of $[BSA]^{-1}$ as per the equation [2].

2.3 Fluorescence Quantum Yield

Fluorescence emission quantum yield of dyes was estimated based on the comparative method reported by Williams et al (21), which involves the use of well characterized standard samples with known Φ_F values.

$$Q = Q_R \left[\frac{Grad}{Grad_R}\right]\left[\frac{\eta^2}{\eta_R^2}\right] \quad [3]$$

Where Q_R is the quantum yield of known (reference) sample, Grad is the gradient obtained from the plot of integrated fluorescence intensity vs. absorbance, Grad is the gradient of reference sample η is the refractive index of the solvent. The fluorescence emission quantum yield assay was done by using different concentrations of dyes ranging from 100 µM to 100 nm in the chloroform as solvent. The electronic absorption and fluorescence emission spectra were recorded. The emission spectra were measured using the corresponding λ_{max} of absorption spectra as the excitation wavelength. Integrated fluorescence intensity (area under the peak) was obtained and a graph between integrated fluorescence intensity vs. absorbance were plotted to obtain straight line with Gradient (m).

2.4 Synthesis of cyanine dyes and intermediates

Model NIR sensitive unsymmetrical cyanine dyes (UCD 1-3) has been synthesized as per the scheme-1 and reported literature procedures.

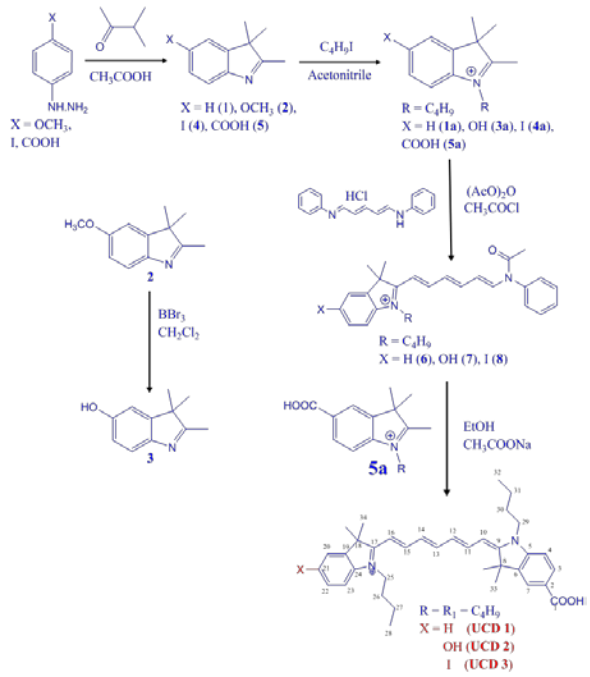

Scheme 1. Synthesis of Unsymmetrical NIR Cyanine dyes.

2.4.1 ***Synthesis of substituted indole derivatives (2, 4, 5)***: The derivatives 5-methoxy-2,3,3-trimethyl-3H-indole (**2**), 5-iodo-2,3,3-trimethyl-3H-indole (**4**) and 2,3,3-trimethyl-3H-indole-5-carboxylic acid (**5**) were Synthesized following the methodology (22-24).

2.4.2 ***Synthesis of 2,3,3-trimethyl-3H-indol-5-ol (3):*** To a solution of compound **2** in dichloromethane (30 mL) at 0°C was added dropwise 2 equivalents of 1 M BBr_3 in dichloromethane and the mixture was stirred at room temperature for 12 hours. Upon the completion of reaction as monitored by thin layer chromatography (TLC), the reaction mixture was washed with saturated aqueous solution of sodium bicarbonate and the organic extracts were dried over Na_2SO_4, filtered, and evaporated to afford **3** as a brown solid in 79% yield (25).

2.4.3 ***Synthesis of Alkyl-3H-indolium iodides (1a-5a):*** The derivatives 1-butyl-2,3,3-trimethyl-3H-indolium iodide (**1a**), 1-butyl-5-hydroxy-2,3,3-trimethyl-3H-indolium (**3a**), 1-butyl-5-iodo-2,3,3-trimethyl-3H-indolium (**4a**) and 1-butyl-5-carboxy-2,3,3-trimethyl-3H-indolium (**5a**) were synthesized by following the procedure (26-29).

2.4.4 ***Synthesis of hemi-cyanine dye (6-8):*** In a round bottom flask one equivalent of corresponding alkyl-3H-indolium iodides (**1a, 3a, 4a,**) and glutaconaldehyde dianil monohydrochloride, along with catalytic amount of acetyl chloride were

dissolved in acetic anhydride. The reaction mixture was refluxed at 140^0C. After the completion of reaction as monitored by TLC, the reaction mixture was poured on to crushed ice to precipitate the desired compound as black solid. This was filtered, dried and purified by silica gel column chromatography (Ethyl acetate: Hexane = 1:1). The titled compound was obtained as red solid (30). 1-butyl-3,3-dimethyl-2-((1E,3E,5E)-6-(N-phenylacetamido)hexa-1,3,5-trien-1-yl)-3H-indolium chloride (**6**) was obtained in 60% yield, MALDI-TOF mass (measured 414.33 $[M+H]^+$; calculated 413.58), 1-butyl-5-hydroxy-3,3-dimethyl-2-((1E,3E,5E)-6-(N-phenylacetamido)hexa-1,3,5-trien-1-yl)-3H-indolium chloride (**7**) obtained in 26% yield, ESI-TOF mass (measured 429.2524 $[M]^+$; calculated 429.2537)1-butyl-5-iodo-3,3-dimethyl-2-((1E,3E,5E)-6-(N-phenyl-acetamido)hexa-1,3,5-trien-1-yl)-3H-indol-1-ium chloride (**8**) obtained in 20% yield confirmed the successful synthesis of intermediate hemi-cyanine's. The ^{1}H-NMR Spectra of these intermediates have been provided in supporting information (figure S3-S5).

2.4.5 ***Synthesis of Unsymmetrical cyanine dyes (UCD 1-3):*** In a round bottom flask one equivalent of corresponding hemi cyanine dye (**6-8**) was dissolved in 20 ml of ethanol. To the above solution one equivalent of Compound **5a** and 2 equivalents of sodium acetate were added. The reaction mixture was refluxed at 95^0C. Upon the completion of reaction as monitored by TLC, the solvent was evaporated under reduced pressure and the residue was dissolved in chloroform and washed with water to remove excess sodium acetate. The organic layer was dried over anhydrous sodium sulphate and evaporated under reduced pressure. The crude product was purified by silica gel column chromatography (Chloroform: Methanol = 9:1) to afford the respective unsymmetrical cyanine dyes as blue green solid (31). The FT-IR spectrum of the dyes have been provided in supporting information (figure S6-S8).

1-butyl-2-((1E,3E,5E)-7-((E)-1-butyl-5-carboxy-3,3-dimethylindolin-2-ylidene)hepta-1,3,5-trien-1-yl)-3,3-dimethyl-3H-indolium chloride (**UCD-1**) was obtained in 10% yield. High resolution (HR)-FAB mass (measured 537.3453 $[M]^+$; calculated 537.3476). ^{1}H NMR (500 MHz $CDCl_3$): 0.99 (6 H, t), 1.26-1.68 (8 H, m), 1.71 (6 H, s), 1.78 (6 H, s), 3.65-4.10 (4H, t), 6.21-6.99 (7 H, m), 7.45 (1 H, s), 7.49 (1 H, s), 7.81 (1 H, s), 7.91 (1 H, s), 8.05-8.13 (3 H, m). ^{13}C NMR (125 MHz, DMSO: δ180.59 (C-17), δ167.16 (C-9), δ166.92 (C-1), δ146.65 (C-6), δ145.67 (C-24), δ142.01 (C-19), δ141.77 (C-5), δ140.30 (C-7), δ136.16 (C-15), δ131.50 (4C, C-11,12,13,14), δ127.60 (C-3, 22), δ125.04 (C-21), δ123.57 (C-20), δ123.06 (C-2), δ122.61 (C-23), δ121.87 (C-4), δ112.34 (C-16), δ109.17 (C-10), δ49.74 (C-8), δ47.21 (C-18), δ43.26 (C-29), δ43.23 (C-25), δ29.52 (C-30), δ28.96 (C-26), δ26.76 (C-33), δ24.12 (C-34), δ19.5 (C-27), δ19.44 (C-31), δ13.78 (C-32), δ13.56

(C-28). FTIR (KBr, cm^{-1}): 2958-m (OH), 1694-s (C=O), 1604-s (C= C), 1515-s (C= C (Ar)), 1417-s (CH_2 bend), 1365-m (C-N), 1316-w (C-O), 833-w (P-substitution), 782-m 714-s (C-H (oop)).

1-butyl-2-((1E,3E,5E)-7-((E)-1-butyl-5-carboxy-3,3-dimethylindolin-2-ylidene)hepta-1,3,5-trien-1-yl)-5-hydroxy-3,3-dimethyl-3H-indolium chloride (UCD-2) obtained in 5% yield. (HR)-ESI - TOF mass (measured 553.3415 [M] +; calculated 553.3425). 1H NMR (500 MHz CDCl3): 0.97 (6 H, t), 1.12-1.58 (8 H, m), 1.65 (6 H, s), 1.69 (6 H, s), 3.99 (2 H, m), 4.44 (2 H, m), 6.10-6.99 (7 H, m), 7.2 (3 H, m), 7.99 (2 H, m), 8.33 (1 H, s). ^{13}C NMR (125 MHz, DMSO: δ177.17 (C-17), δ170.09 (C-9), δ166.18 (C-1), δ153.49 (C-6), δ149.34 (C-24), δ144.94 (C-19), δ140.79 (C-5), δ132.49 (C-15), δ131.75 (C-11,12,13,14), δ129.92 (C-3, 22), δ126.99 (C-7), δ123.57 (C-21), δ122.11 (C-20), δ120.89 (C-2), δ104.77 (C-23), δ98.67 (C-4), δ95.74 (C-10), δ93.05 (C-16), δ58.26 (C-18), δ48.73 (C-25), δ44.34 (C-8), δ42.38 (C-29), δ29.69 (C-26), δ28.22 (C-30), δ25.54 (C-33), δ24.80 (C-34), δ20.41 (C-27), δ20.16 (C-31), δ15.29 (C-32), δ14.55 (C-28).FTIR (KBr, cm-1): 2964-m (OH), 1695-m (C=O), 1605-s (C= C), 1521-m (C= C (Ar)), 1417-m (CH2 bend), 1360-s (C-N), 1291-w (C-O (carboxyl)), 1091-s (C-O), 831-w (p-substitution), 716-s (m-substitution), 658-w (C-H (oop)).

1-butyl-2-((1E,3E,5E)-7-((E)-1-butyl-5-carboxy-3,3-dimethylindolin-2-ylidene)hepta-1,3,5-trien-1-yl)-5-iodo-3,3-dimethyl-3H-indolium chloride (**UCD-3**) obtained in 11 % yield. ^{1}H NMR (500 MHz $CDCl_3$): 0.97 (6 H, t), 1.1-1.58 (8 H, m), 1.65 (6 H, s), 1.69 (6 H, s), 4.0-4.10 (4H, m), 6.2-7.2 (7 H, m), 7.55 (1 H, s), 7.63 (2 H, d), 7.99 (1 H, s), 8.09 (2 H, d). ^{13}C NMR (125 MHz, DMSO: δ176.20 (C-17), δ173.70 (C-9), δ168.09 (C-1), δ154.23 (C-5), δ147.10 (C-24), δ146.47 (C-19), δ145.07 (C-6), δ140.91 (C-15), δ133.14 (C-14), δ132.69 (C-13), δ131.68 (C-12), δ129.62 (C-11), δ125.78 (C-7), δ124.06 (C-3, 22), δ123.70 (C-21), δ122.37 (C-20), δ121.87 (C-2), δ119.29 (C-23), δ113.63 (C-4), δ112.14 (C-10), δ86.92 (C-16), δ69.18 (C-18), δ63.35 (C-25), δ48.29 (C-8), δ44.65 (C-29), δ29.89 (C-26), δ29.87 (C-30), δ27.98 (C-33), δ24.44 (C-34), δ20.36 (C-27), δ20.13 (C-31), δ14.35 (C-32), δ14.20 (C-28). FTIR (KBr, cm^{-1}): 2958-m (OH), 1699-m (C=O), 1605-m (C= C), 1506-s (C= C (Ar)), 1415-s (CH_2 bend), 1360-s (C-N), 1309-w (C-O (carboxyl)), 816-w (p-substitution), 714-s (m-substitution), 649-m (C-H (oop)), 554-w (C-I).

3. Results and Discussion

3.1 Photophysical Characterization

After the successful synthesis and purification these NIR sensitive dyes were subjected to photophysical investigations pertaining to the electronic absorption and fluorescence emission spectroscopy. Results thus obtained pertaining to the photophysical parameters have been summarized in the table 1. Figure 1 exhibits the solution state

electronic absorption and fluorescence emission spectra for the unsymmetrical cyanine dyes in the dimethylformamide (DMF) solution.

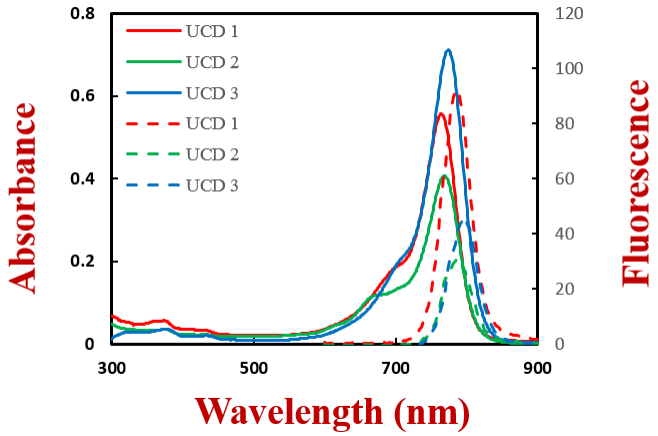

Fig.1. Electronic absorption (solid line) and fluorescence emission (dashed line) spectra of UCD 1-3 in DMF solution (5 μM).

It can be observed that position of maxima (λ_{max}) for the electronic absorption and fluorescence emission in DMF are not much affected by the different substituents (hydroxyl and iodo) present in main π-conjugated polymethene framework. The λ_{max} of unsymmetrical cyanine dyes ranges from 764 to 774 nm with high molar extinction coefficients ($\varepsilon \approx 10^5$ dm^3 M^{-1} cm^{-1}). This sharp and intense light absorption in this class of dyes is associated with the π–π* electronic transitions. The fluorescence emission spectra for each of dyes were measured slightly below (about 15-20 nm) to the corresponding λ_{max} of absorption spectrum as the excitation wavelength. For all of the unsymmetrical cyanine dyes one main emission band can be observed which is ranging from 788 nm to 798 nm, with a small Stokes shift of 23 and 24 nm. This small Stokes shift represents the rigidity of the molecules without having any conformational changes after the photoexcitation.

Table 1. Spectral properties of dyes in DMF and 0.1 M PBS solution at pH 7.4.

DYE	DMF Solution				PBS Solution	
	λ (max) Absorption	λ (max) Emission	Stoke Shift	(ε) (dm^3 M^{-1} cm^{-1})	λ (max) Absorption	Quantum Yield
UCD -1	764 nm	788 nm	24 nm	1.1×10^5	749 nm	0.327
UCD -2	769 nm	792 nm	23 nm	0.8×10^5	753 nm	0.196
UCD -3	774 nm	798 nm	24 nm	1.4×10^5	757 nm	0.649

To investigate the interactions between the dyes and the biomolecules for imaging applications, Phosphate buffer solution (PBS) has been most commonly used. Keeping this in mind, electronic absorption spectra of these dyes were also measured in the 0.1 M PBS solution at pH 7.4 which has been shown in the figure 2. It is worth mentioning that the absorption spectra of cyanine dyes in PBS exhibited slightly blue shifted λ_{max} compared to that observed in DMF. This behaviour of blue shifted λ_{max} could be attributed to the enhancement in aggregation of dye, promoted by the hydrogen bonding between the dye molecules due to the presence of –COOH groups. It is well known that cyanine dyes exhibit dye aggregation owing to their flat molecular structure (32). Apart from the main π-π* electronic transition, cyanine and squaraine dyes also exhibit a vibronic shoulder just before the main absorption peak and the vibronic shoulder has been reported to be marker of molecular aggregation (33). Higher value of the ratio of absorbance for the vibronic shoulder with respect to the absorbance corresponding to the main π-π* transition indicates an enhanced dye aggregation (34, 35).

A perusal of absorption spectra shown in the Fig. 2 clearly corroborates that vibronic shoulders of the dyes in PBS are relatively more pronounced as compared to that observed in the DMF (Fig. 1) verifying the enhanced dye aggregation and this could be attributed to the blue-shifted λ_{max} also. It is interesting to mention here that amongst all of the unsymmetrical squaraine dyes used in this work UCD-2 exhibits relatively enhanced dye aggregation due to prominent vibronic shoulder which was visible even in the DMF solution (Fig. 1) and becomes even more prominent in the PBS. This could be attributed to the fact that apart from –COOH functional group which is present in all of the dyes, it bears –OH substituted at the 5-position of the other indole ring which is expected to enhance the hydrogen bond assisted enhanced dye aggregation.

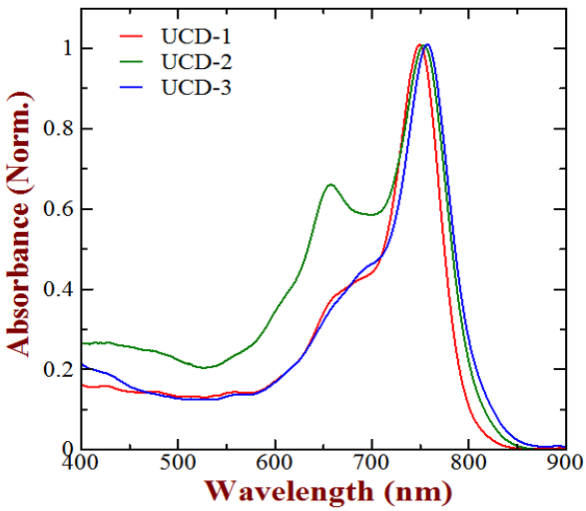

Fig. 2. Electronic absorption spectra for unsymmetrical cyanine dyes UCD 1-3 in 0.1 M PBS.

Fluorescence quantum yield (ϕ) is an important parameter towards the development of fluorescent probes and is an indicator of the capability of a fluorescent probe to convert absorbed photons in to the emitted one in a particular environment. In combination with molar extinction coefficient (ε) it signifies the strength of fluorescence signal since product of the ϕ and ε determines the brightness of fluorophore. A perusal of table 1 indicates that newly synthesized dyes in this work exhibits moderate the high ϕ values compared to that of the values reported for a variety of typical NIR cyanine dyes. A perusal of the ϕ calculated for different unsymmetrical cyanine dyes as indicated in the table 1 indicates that they exhibit fairly good values as compared to typical NIR cyanine dyes. Amongst the dyes used in this work, it can be seen that –OH substituted cyanine dye UCD-2 exhibits relatively hampered value of ϕ (about 0.20) as compared to the unsubstituted UCD-1(0.33). This could be attributed the fact that UCD-2 exhibits pronounced aggregate formation and aggregate assisted non-radiative fluorescence decay leading to the hampered ϕ.

3.2 Interaction of Dyes with Bovine Serum Albumin

In order to avoid the purification steps in labelling of biomolecules with dyes towards the application of optical bio imaging, non-covalent methods have been frequently used (36). Patonay and co-workers were among the first to study the noncovalent labelling of the human serum albumin (HSA) with near-infrared dyes by using high-performance liquid chromatography (HPLC) and absorption detection (37). At the same time, bovine serum albumin (BSA) is a globular protein which has been prominently used as protein model to investigate the interactions between dye and protein owing to its high homology with HSA in the amino acidic sequences (38). Therefore, dyes used in this work have also been subjected to investigate their interaction with the BSA as a model protein. Figure 3 depicts the absorption spectra of one of the representative cyanine dyes (UCD-1) in the presence and absence of BSA. It can be seen that there are two different sets of prominent electronic absorption bands in the wavelength region of 250 nm - 300 nm and 700 nm - to 800 nm associated with the absorption of BSA and dye UCD-1, respectively. Increase in the BSA concentration led to the gradual increase in intensity of absorption between 250 nm - 300 nm, which was associated with electronic absorption of the protein BSA.

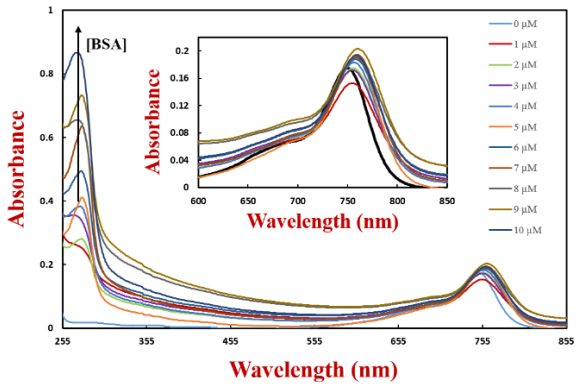

Fig. 3. Electronic absorption spectra of UCD 1 in 0.1 M PBS at different concentrations of BSA for fixed dye concentration of 2 µM.

However, there was random increase and decrease of absorption intensity associated with dye in NIR region of 600 nm - 800 nm, a behaviour similar to that observed by Pisoni et al also (26). At the same time, random increase and decrease without any isobestic point indicates that the equilibrium between the free and bound protein is not simple in all the dyes under investigation. Interestingly, λ_{max} associated with UCD-1 which was around 750 nm in the absence of BSA was found to be bathochromically shifted by 5-10 nm in the presence of BSA. This could be attributed to the suppression of dye aggregation due to the interactions between the protein and dye molecules. Similar type of behaviour has also been observed for the other cyanine dyes (UCD-2 and UCD-3) and results have been provided in the supporting information (Figure S1-S2).

The fluorescence emission spectra of UCD-1 in the presence and absence of BSA is shown in the Fig. 4. It can be seen that dye exhibits increase in fluorescence intensity near the λ_{max} along with slight red shift of peak maxima upon the addition of increasing amounts of BSA. The increase in fluorescence intensity could be attributed to the possible interaction between the UCD-1 and BSA.

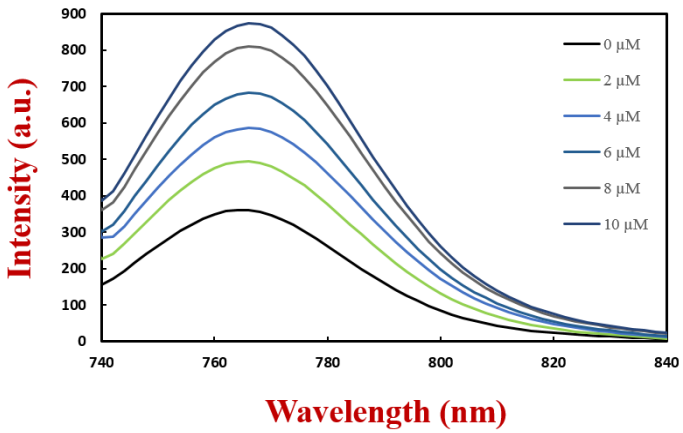

Fig. 4. Fluorescence emission spectra of UCD-1 with varying concentrations of BSA for a fixed dye concentration of 2 µM.

This interaction may lead to the strengthening of the planar configuration of the dye molecules especially in the excited state ultimately enhancing the molecular rigidity after formation of complex between UCD-1 and BSA. It seems quite probable that –COOH functionality of dye is expected to the hydrogen bond assisted dye aggregate formation in PBS leading to the blue-shifted emission maximum (Table 1). In the presence of BSA in the PBS this aggregate formation is hampered due to the dye-BSA complex formation leading to bathochromically shifted emission. For the other dyes under investigation also electronic absorption and fluorescence emission spectra in the presence and absence of BSA were also measured and shown in the supporting information (Fig. S1-S2).

Here one can argue that during the interaction of BSA with dyes under investigation is there any detrimental effects like denaturation of BSA with dyes. To have the in-depth insight about this we have conducted the measurement of circular dichroism (CD) of the BSA in the presence and absence of the dyes and obtained results of the measurement have been shown in the Fig. 5. The CD spectrum of BSA was taken by adjusting concentration of BSA to 5 μM in PBS while the CD spectrum of BSA-dye solutions were executed with 0.2 μM dye and 5 μM BSA. It is well known that CD spectrum of BSA typically consists of two negative bands appearing at 208 nm and 222 nm associated with the $n \rightarrow \pi^*$ transition and negative Cotton effect, respectively (39-40). BSA contains the distinct binding domains for hydrophobic compounds. The specific interactions of dye by BSA originates from the presence of two structurally selective binding sites, namely site I and site II. The binding affinity offered by site I is purely hydrophobic interactions where as the site II involves a combination of hydrophobic, hydrogen bonding and electrostatic interactions (41). A perusal of the Fig. 5 pertaining to the CD spectra clearly reveals the persistence of both of negative bands of BSA around 208 nm and 222 nm in the presence of all of the dyes under investigation which depicts that there is no denaturation of the BSA in the presence of dyes.

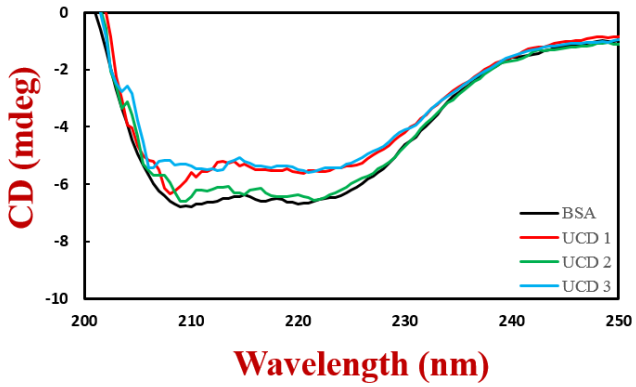

Fig. 5. CD spectra of BSA and dye-BSA complexes at pH 7.4.

BSA concentration dependence of the fluorescence intensity for various unsymmetrical cyanine dyes have been shown in the Fig. 6. A linear correlation between fluorescent intensity of dyes as a function of BSA concentration was observed. This increase in fluorescent intensity along with red shift of λ_{max} can be attributed to the non-covalent interaction between dyes and protein for the formation of BSA-dye conjugates.

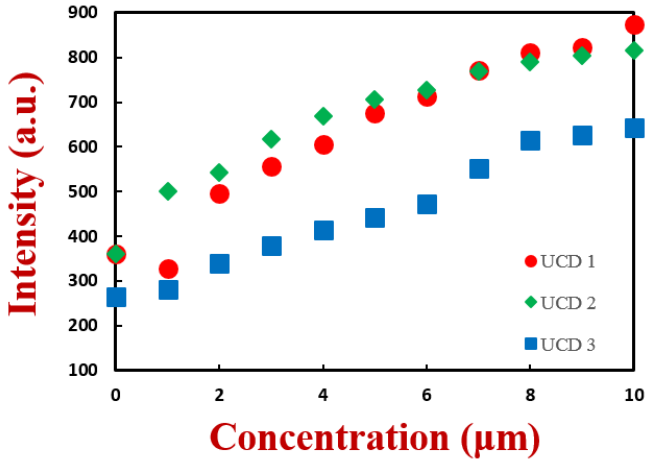

Fig. 6. Plot of florescence emission intensity at peak maxima for cyanine dyes (UCD 1-4) as a function of BSA concentration. Dye concentration was constant (2 µM) for each of the dyes.

It has been widely accepted that drugs or probes interact differently with the protein under consideration and their ability to bind depends on protein concentration (25). It can be clearly seen that ability to bind with fluorescent dyes utilized in this work were enhanced upon the addition of increasing concentration of BSA. At the same time, amongst the dyes utilized dye-BSA interaction studies, UCD-3 was found to exhibit the highest binding affinity BSA. In order to successfully implement fluorescent dyes as a probe, it is necessary that the dye should bind to the protein without causing any damage to its three dimensional conformation which basically governs the protein function and activity. The conformational changes in protein may occur at the point where probe is located. As the dye concentration increases, there may be more damage in its activity. Keeping this mind, a very low dye concentration of (2 µM) has been used for investigation of the dye-BSA interaction with all of the unsymmetrical NIR cyanine dyes. Thanks to high ε and good ϕ of the dyes, it possible to investigate the interaction satisfactorily even at lower dye concentration.

To compare the ability of binding and relative association of dyes with BSA quantitatively, apparent binding constant (K_a) was calculated using equation [2] by plotting $(F\infty - F_0)/(F_X - F_0)$ as function of inverse of BSA concentration as shown in the Fig. 7. The value of K_a was calculated from the slopes of the this figure which was found to be 7.08×10^6 M^{-1}, 3.7×10^6 M^{-1} and 10.13×10^6 M^{-1} with the cyanine dyes UCD-1, UCD-2 and UCD-3, respectively. Therefore, unsymmetrical cyanine dye bearing 5-Iodoindole exhibits highest binding affinity with the BSA and estimated K_a is about an order of the magnitude higher as compared to that obtained for the typical cyanine dyes (27). This could be attributed to the presence of direct ring substituted hydrophilic carboxylic acid (–COOH) functional group promoting hydrogen bonding with binding sites of BSA.

As discussed earlier BSA possess distinct hydrophobic and hydrophilic active sites (Site I and Site-II). Upon interaction with the ligands (drug or dyes) the relative hydrophobicity of ligands plays an important role in controlling their interactions with the BSA specifically with Site-I. A perusal of the molecular structures of the dyes under investigation reveals that all of dyes possess nearly same main p-framework, alkyl group and –COOH functional group apart from the varying substituents (-OH, H or –I) in the main aromatic ring at the other terminal indole unit. Since other structural factors are constant, UCD-3 exhibits relatively more hydrophobic nature as compared to the UCD-2 bearing –OH group which is responsible for its enhanced interaction with BSA ultimately leading to high binding ability. On the other hand enhanced aggregation and competitive interactions due to presence of two functional groups –OH and –COOH on the two opposite ends of the chromophore in the dye UCD-2 could be attributed to the least association with the BSA.

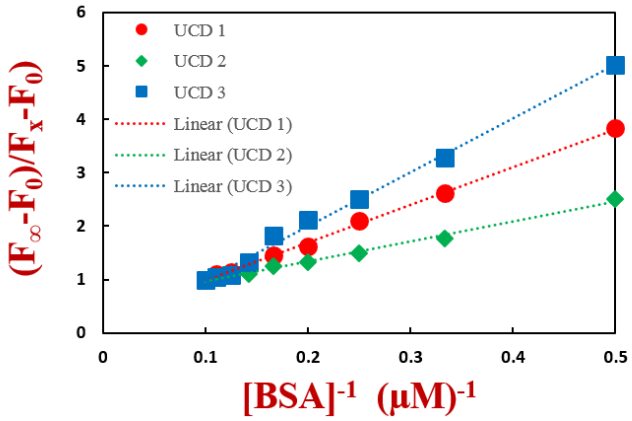

Fig. 7. Plot of $(F\infty - F_0)/(F_X - F_0)$ as function $[BSA]^{-1}$ at a fixed dye concentration of 2.0×10^{-6} M.

4. Conclusions

Direct ring carboxy functionalized NIR sensitive unsymmetrical cyanine dyes having different substituents (-OH and -I) have been successfully synthesized and characterized. These dyes were subjected to the photophysical investigations in order to explore their applicability as fluorescent probes. Interactions of these dyes with BSA as a protein model suggested the formation of dye-BSA conjugates, which led to the enhancement in fluorescence intensity along with bathochromic shift of emission maxima. Amongst the various dyes utilized, one with mild electron withdrawing iodo group (UCD-3) has been found to exhibit the highest affinity towards the association with BSA. This high binding constant observed in the case of UCD-3 could be associated with the presence of relatively bulkier iodo group along with the –COOH group directly attached with the indole ring.

Acknowledgements

Authors would like to acknowledge the support from Prof. Shigeori Takenaka (Kyushu Institute of Technology, Tobata) in obtaining Mass spectra and Jelli Venkata Prasad in obtaining H-NMR Spectra.

References

1. Licha K, Riefke B, Ebert B, Grötzinger C. Cyanine dyes as contrast agents in biomedical optical imaging. Academic radiology. 2002;9(2):S320-S2.
2. Rao J, Dragulescu-Andrasi A, Yao H. Fluorescence imaging in vivo: recent advances. Current opinion in biotechnology. 2007;18(1):17-25.
3. Nizomov N, Ismailov Z, Kurtaliev E, Nizamov SN, Khodzhaev G, Patsenker L. Luminescent spectral properties of rhodamine derivatives while binding to serum albumin. Journal of Applied Spectroscopy. 2006;73(3):432-6.
4. Yuan L, Lin W, Zhao S, Gao W, Chen B, He L, et al. A Unique Approach to Development of Near-Infrared Fluorescent Sensors for in Vivo Imaging. Journal of the American Chemical Society. 2012;134(32):13510-23.
5. Patonay G, Antoine MD. Near-infrared fluorogenic labels: New approach to an old problem. Analytical Chemistry. 1991;63(6):321A-7A.
6. Frangioni JV. In vivo near-infrared fluorescence imaging. Current opinion in chemical biology. 2003;7(5):626-34.
7. Hawrysz DJ, Sevick-Muraca EM. Developments Toward Diagnostic Breast Cancer Imaging Using Near-Infrared Optical Measurements and Fluorescent Contrast Agents 1. Neoplasia. 2000;2(5):388-417.
8. Ntziachristos V, Bremer C, Weissleder R. Fluorescence imaging with near-infrared light: new technological advances that enable in vivo molecular imaging. European radiology. 2003;13(1):195-208.
9. Yagi S, Nakasaku Y, Maeda T, Nakazumi H, Sakurai Y. Synthesis and near-infrared absorption properties of linearly π-extended squarylium oligomers. Dyes and Pigments. 2011;90(2):211-8.
10. Yang X, Shi C, Tong R, Qian W, Zhau HE, Wang R, et al. Near IR heptamethine cyanine dye–mediated cancer imaging. Clinical Cancer Research. 2010;16(10):2833-44.
11. Law KY. Squaraine chemistry. Design, synthesis and xerographic properties of a highly sensitive unsymmetrical fluorinated squaraine. Chemistry of materials. 1992;4(3):605-11.
12. Escobedo JO, Rusin O, Lim S, Strongin RM. NIR dyes for bioimaging applications. Current opinion in chemical biology. 2010;14(1):64-70.
13. Mishra A, Behera RK, Behera PK, Mishra BK, Behera GB. Cyanines during the 1990s: a review. Chemical Reviews. 2000;100(6):1973-2012.
14. Yuan L, Lin W, Zheng K, He L, Huang W. Far-red to near infrared analyte-responsive fluorescent probes based on organic fluorophore platforms for fluorescence imaging. Chemical Society Reviews. 2013;42(2):622-61.
15. El-Shishtawy RM. Functional dyes, and some hi-tech applications. International Journal of Photoenergy. 2009;2009.
16. Benzi C, Bertolino CA, Miletto I, Ponzio P, Barolo C, Viscardi G, et al. The design, synthesis and characterization of a novel acceptor for real time polymerase chain reaction using both computational and experimental approaches. Dyes and Pigments. 2009;83(1):111-20.

17. Tatikolov AS, Costa SlM. Complexation of polymethine dyes with human serum albumin: a spectroscopic study. Biophysical chemistry. 2004;107(1):33-49.
18. Reddington MV. Synthesis and properties of phosphonic acid containing cyanine and squaraine dyes for use as fluorescent labels. Bioconjugate Chemistry. 2007;18(6):2178-90.
19. Gonçalves MST. Fluorescent labeling of biomolecules with organic probes. Chemical reviews. 2008;109(1):190-212.
20. ZHANG YZ, YANG QF, DU HY, TANG YL, XU GZ, YAN WP. Spectroscopic investigation on the interaction of a cyanine dye with serum albumins. Chinese Journal of Chemistry. 2008;26(2):397-401.
21. Williams ATR, Winfield SA, Miller JN. Relative fluorescence quantum yields using a computer-controlled luminescence spectrometer. Analyst. 1983;108(1290):1067-71.
22. Li H, Pang M, Wu B, Meng J. Synthesis, crystal structure and photochromism of a novel spiro [indoline–naphthaline] oxazine derivative. Journal of Molecular Structure. 2015;1087:73-9.
23. Klotz EJ, Claridge TD, Anderson HL. Homo-and hetero-[3] rotaxanes with two π-systems clasped in a single macrocycle. Journal of the American Chemical Society. 2006;128(48):15374-5.
24. Inoue T, Pandey SS, Fujikawa N, Yamaguchi Y, Hayase S. Synthesis and characterization of squaric acid based NIR dyes for their application towards dye-sensitized solar cells. Journal of Photochemistry and Photobiology A: Chemistry. 2010;213(1):23-9.
25. Oushiki D, Kojima H, Takahashi Y, Komatsu T, Terai T, Hanaoka K, et al. Near-infrared fluorescence probes for enzymes based on binding affinity modulation of squarylium dye scaffold. Analytical chemistry. 2012;84(10):4404-10.
26. Pisoni DS, Todeschini L, Borges ACsA, Petzhold CL, Rodembusch FS, Campo LF. Symmetrical and Asymmetrical Cyanine Dyes. Synthesis, Spectral Properties, and BSA Association Study. The Journal of organic chemistry. 2014;79(12):5511-20.
27. Oshikawa Y, Furuta K, Tanaka S, Ojida A. Cell Surface-Anchored Fluorescent Probe Capable of Real-Time Imaging of Single Mast Cell Degranulation Based on Histamine-Induced Coordination Displacement. Analytical Chemistry. 2016.
28. Gerowska M, Hall L, Richardson J, Shelbourne M, Brown T. Efficient reverse click labeling of azide oligonucleotides with multiple alkynyl Cy-Dyes applied to the synthesis of HyBeacon probes for genetic analysis. Tetrahedron. 2012;68(3):857-64.
29. Pandey SS, Inoue T, Fujikawa N, Yamaguchi Y, Hayase S. Substituent effect in direct ring functionalized squaraine dyes on near infra-red sensitization of nanocrystalline TiO 2 for molecular photovoltaics. Journal of Photochemistry and Photobiology A: Chemistry. 2010;214(2):269-75.
30. Berezin MY, Guo K, Teng B, Edwards WB, Anderson CJ, Vasalatiy O, et al. Radioactivity-synchronized fluorescence enhancement using a radionuclide fluorescence-quenched dye. Journal of the American Chemical Society. 2009;131(26):9198-200.
31. Redy O, Kisin-Finfer E, Sella E, Shabat D. A simple FRET-based modular design for diagnostic probes. Organic & biomolecular chemistry. 2012;10(4):710-5.
32. Tatikolov AS. Polymethine dyes as spectral-fluorescent probes for biomacromolecules. Journal of Photochemistry and Photobiology C: Photochemistry Reviews. 2012;13(1):55-90.
33. Peyratout C, Daehne L. Aggregation of thiacyanine derivatives on polyelectrolytes. Physical Chemistry Chemical Physics. 2002;4(13):3032-9.
34. Behera G, Behera P, Mishra BK. Cyanine Dyes: Self Aggregation and Behaviour in Surfactants A Review. Journal of Surface Science and Technology. 2007;23(1/2):1.
35. Shivashimpi GM, Pandey SS, Hayat A, Fujikawa N, Ogomi Y, Yamaguchi Y, et al. Far-red sensitizing octatrifluorobutoxy phosphorous triazatetrabenzocorrole: Synthesis, spectral characterization and aggregation studies. Journal of Photochemistry and Photobiology A: Chemistry. 2014;289:53-9.
36. Patonay G, Salon J, Sowell J, Strekowski L. Noncovalent labeling of biomolecules with red and near-infrared dyes. Molecules. 2004;9(3):40-9.

37. Williams RJ, Lipowska M, Patonay G, Strekowski L. Comparison of covalent and noncovalent labeling with near-infrared dyes for the high-performance liquid chromatographic determination of human serum albumin. Analytical chemistry. 1993;65(5):601-5.
38. Turbay MBE, Rey V, Argañaraz NM, Vieyra FEM, Aspée A, Lissi EA, et al. Effect of dye localization and self-interactions on the photosensitized generation of singlet oxygen by rose bengal bound to bovine serum albumin. Journal of Photochemistry and Photobiology B: Biology. 2014;141:275-82.
39. Yang P, Gao F. The principle of bioinorganic chemistry. Science, Beijing. 2002;349.
40. Greenfield NJ, Fasman GD. Computed circular dichroism spectra for the evaluation of protein conformation. Biochemistry. 1969;8(10):4108-16.
41. Jiménez MC, Miranda MA, Vayá I. Triplet excited states as chiral reporters for the binding of drugs to transport proteins. Journal of the American Chemical Society. 2005;127(29):10134-5.